Catalysis Today 150 (2010) 218–223

Contents lists available at ScienceDirect

Catalysis Today

journal homepage: www.elsevier.com/locate/cattod

Hydrodesulfurization of dibenzothiophene catalyzed by Pd supported on overgrowth-type MCM-41/HY composite

Feng Zhou [a], Xiang Li [a,b], Anjie Wang [a,b,*], Linying Wang [a], Xiaodong Yang [a], Yongkang Hu [a]

[a] State Key Laboratory of Fine Chemicals, Dalian University of Technology, 158 Zhongshan Road, Dalian 116012, PR China
[b] Liaoning Key Laboratory of Petrochemical Technology and Equipments, Dalian University of Technology, Dalian 116012, PR China

ARTICLE INFO

Article history:
Available online 3 September 2009

Keywords:
MCM-41
HY
Composite
Pd
Hydrodesulfurization

ABSTRACT

Siliceous MCM-41 (Si-MCM-41), aluminosilicate MCM-41 (Al-MCM-41) and two micro-mesoporous materials obtained either by physically mixing Si-MCM-41 with HY zeolite [MY(M)] or by overgrowing Si-MCM-41 over HY zeolite particles [MY(C)], were prepared and characterized by means of XRD, XRF and pyridine adsorbed FT-IR. The hydrodesulfurization (HDS) performances of the supported Pd catalysts were evaluated with dibenzothiophene (DBT) as the model sulfur-containing molecule. The results indicated that the HDS performances of Pd catalysts are significantly influenced by the pore structures and acid properties of the supports. Pd catalysts supported on the acidic supports showed enhanced stability as well as HDS and hydrogenation (HYD) activities. Among the catalysts studied, Pd/MY(C) exhibited the highest activity and stability in DBT HDS. Its enhanced HDS performance especially sulfur resistance may result from the unique core/shell structure of MY(C). The effect of the acid properties and pore structures of the supports on the HDS performances of Pd catalysts was discussed by considering formation of "electronic-deficient" Pd particles and an "auto-regeneration" mechanism involving spillover hydrogen.

Among all sulfur-containing compounds present in diesel, dibenzothiophene (DBT) and its alkylated derivatives like 4-methyl-dibenzothiophene (4-MDBT) and 4,6-dimethyl-dibenzothiophene (4,6-DMDBT) are the most refractory sulfur-containing molecules to desulfurize due to steric hindrance [1,2]. Therefore, hydrogenation of the neighboring aromatic rings of these molecules to relieve the steric hindrance is required before desulfurization [3]. Due to high hydrogenation ability, the supported noble metal catalysts are good candidates for deep hydrodesulfurization (HDS) aiming at removing these highly refractory sulfur-containing compounds [4–7]. Nevertheless, the HDS activity of noble metals is not stable, because they are readily to be transformed into their sulfides in the presence of H_2S. As a consequence, unless noble metal catalysts are proven to withstand the preferable stability or thioresistance towards sulfur-containing feed, they will still be of limited use in deep HDS.

The sulfur tolerance of noble metal catalysts can be improved by alloying [8,9], adding a second metal [10,11], or optimizing the support. It is well known that the sulfur tolerance [9,12] and the intrinsic activity [13,14] of the noble metal catalysts can be improved by supporting them on acidic supports. As important acidic components, zeolite or zeolite-containing supports have attracted much attention. Nevertheless, their small pore size means that relatively large molecules such as DBT and 4,6-DMDBT cannot enter the pores and reach the active sites inside. Moreover, their excessively strong acidity can result in strong hydrocracking activity, lowering the liquid yields, as well as inducing severe deactivation by coking [7]. Therefore, a support with relatively large pores and optimized acid site distributions would be preferred. Dealuminized zeolites [9,15], mesoporous zeolites [6,16] and microporous and mesoporous composite materials [17–19] will open the possibility to prepare highly active and sulfur-resistant noble metal catalysts in the deep HDS of bulky organosulfur compounds.

In our previous work, we synthesized an overgrowth-type MCM-41/HY micro-mesoporous composite [20]. The material has unique core/shell structures, in which HY zeolite is coated by an MCM-41 layer and the MCM-41 pore channels are oriented outward from the inner HY core. The supported NiMo sulfides exhibited superior HDS activity and low hydrocracking activity [20,21]. In the present work, to gain further insight into the influence of the pore structure of the support on the HDS activities,

* Corresponding author at: School of Chemical Engineering, Dalian University of Technology, Dalian 116012, PR China. Tel.: +86 411 39893693; fax: +86 411 39893693.
E-mail address: ajwang@chem.dlut.edu.cn (A. Wang).

0920-5861/$ – see front matter © 2009 Elsevier B.V. All rights reserved.
doi:10.1016/j.cattod.2009.07.092

selectivities and stabilities of supported Pd catalysts, the HDS performances of Pd catalysts supported on the overgrowth-type MCM-41/HY composite as well as siliceous MCM-41 (Si-MCM-41), aluminosilicate MCM-41 (Al-MCM-41) and the physical mixture of Si-MCM-41 and HY zeolite were studied using DBT as the model sulfur-containing molecule.

1. Experimental

1.1. Materials

Sodium silicate hydrate, cetyltrimethylammonium bromide (CTABr), aluminium sulfate [$Al_2(SO_4)_3$] and palladium chloride ($PdCl_2$) were all of A.R. grade. Dibenzothiophene (DBT) was synthesized using biphenyl and sulfur according to the method in the literature [22]. Decalin was a product of Shanghai Chemical Reagents Co. and used as solvent without further purification. Zeolite HY (SiO_2/Al_2O_3 ratio: 5, unit cell: 2.47 nm) was provided by Fushun Research Institute of Petroleum and Petrochemicals, China. A cylinder of H_2 was supplied by Dalian Institute of Chemical Physics Special Gas Co. Prior to being introduced into the reactor, the H_2 was deoxygenated by flowing through a tiny catalyst bed and then dried through an adsorption bed.

1.2. Support and catalyst preparation

Siliceous MCM-41 (denoted as Si-MCM-41) and aluminosilicate MCM-41 (denoted as Al-MCM-41) were prepared following the procedure reported previously using CTABr as the template as well as sodium silicate hydrate and aluminium sulfate as the silica and aluminium source, respectively [23]. The overgrowth-type composite was synthesized by overgrown mesoporous Si-MCM-41 over HY zeolite crystals according to the recipe given in [20]: 4.25 g of CTABr was dissolved in 40 ml of de-ionized water, and 1.2 g of HY was added to the solution at 25 °C and stirred for 24 h to form slurry A. Solution B was prepared by dissolving 16.5 g of sodium silicate hydrate in 100 ml of de-ionized water, and the pH was adjusted to 11 by adding 6 M H_2SO_4. After being stirred for 10 min, slurry A was added dropwise to solution B. The obtained gel mixture was agitated at room temperature for 2 h, and then charged in an autoclave which was kept at 120 °C for 48 h. After the hydrothermal reaction, the solid product was separated by filtration, followed by washing, drying, and calcination at 540 °C for 6 h. The obtained composite is denoted as MY(C). The content of HY in the MY(C) was estimated from the weight of HY zeolite and the total weight of the synthesized composite to be around 25 wt.%. For comparison, the physical mixture of Si-MCM-41 and HY zeolite with the same HY content (25 wt.%) was prepared by milling in a mortar, and it is denoted as MY(M).

Pd catalysts supported over Si-MCM-41, Al-MCM-41, MY(M), and MY(C) were prepared by impregnating the support in an appropriate dilute hydrochloric acid solution of $PdCl_2$ for 8 h at room temperature (25 °C), followed by drying at 120 °C overnight and calcination at 500 °C in air for 3 h. For each catalyst, the loading level of Pd was 1 wt.%. The resulting catalysts are nominated as Pd/Si-MCM-41, Pd/Al-MCM-41, Pd/MY(M) and Pd/MY(C).

1.3. Characterization

The X-ray diffraction (XRD) patterns of the supports were measured on a Rigaku D/MAX-2400 diffractometer using nickel-filtered CuKα radiation at 40 kV and 100 mA. Nitrogen adsorption–desorption measurements were performed using an ASAP 2010 adsorption analyzer. The sample was outgassed for 4 h at 300 °C prior to adsorption. The SiO_2/Al_2O_3 ratios of the supports were determined by means of an XRF analyzer (RSR 3400 X). The pyridine adsorbed FT-IR spectra were recorded using an equinox55 spectrophotometer. Before the pyridine adsorption experiment, the sample was subjected to vacuum in the sample holder at 450 °C for 4 h until a pressure of 7×10^{-4} Pa was reached. Pyridine vapor was added in doses at ambient temperature until the catalyst surface was saturated, and then desorbed until a pressure of 7×10^{-4} Pa was reached to ensure that there was no more physisorbed pyridine on the sample. The sample containing chemisorbed pyridine was subjected to thermal treatment at 300 °C and then the IR spectrum was recorded.

1.4. HDS of DBT

The HDS of DBT was conducted in a trickle bed stainless-steel tubular reactor (8.0-mm i.d.). Catalyst samples were pelleted and then crushed and screened to 20–35 meshes. To improve the thermal conductivity, 0.05 g of catalyst diluted with 1.8 g of inert particles of quarts sand was charged for each run. The HDS activities of the prepared catalysts were evaluated with 0.8 wt.% DBT in decalin as the model fuel. Prior to HDS reaction, the catalyst was reduced at 300 °C and 1 MPa with a 30 N ml/min hydrogen flow for 2 h. After that, the total pressure was increased to 5.0 MPa by H_2. The reaction conditions for the HDS of DBT were: temperature 300 °C, total pressure 5.0 MPa, H_2/feed ratio 850 N m^3/m^3, and WHSV 54 h^{-1}. The reaction products were introduced into a gas–liquid separator to collect the liquid products. The feed and liquid products were analyzed by an Agilent 6890N gas chromatograph equipped with an FID detector using a commercial HP-5 column.

The HDS of DBT proceeds through two parallel pathways: the direct desulfurization pathway (DDS) and the hydrogenation pathway (HYD). Biphenyl (BP) is the only product of DDS pathway. The HYD pathway leads to the formation of DBT hydrogenated intermediates, such as tetrahydrodibenzothiphene (TH-DBT) and hexahydrodibenzothiophene (HH-DBT), as well as their desulfurized products (cyclohexylbenzene (CHB) and bicyclohexyl (BCH)). Over acidic catalysts, the hydrocracking (HYC) of CHB and BCH may take place, producing benzene, cyclohexane and the other hydrocarbons with the carbon number no more than 6.

Because the transformation of BP to CHB is negligible in the presence of DBT, BP selectivity (S_{BP}) is used as a measure of the DBT DDS pathway selectivity, while ($1 - S_{BP}$) represents the selectivity to the HYD pathway [21]. The products over acidic materials supported Pd catalysts in HDS of DBT are complex, including DBT hydrogenated intermediates, desulfurized molecules and hydrocracking products. Therefore, HDS conversion (x_{HDS}) and HYC conversion (x_{HYC}) were used to present the desulfurization and hydrocracking activity of supported Pd catalysts respectively, which were calculated as:

$$x_{HDS} = \frac{C_0 - C_{DBT} - C_{TH} - C_{HH}}{C_0} \times 100\% \quad (1)$$

$$x_{HYC} = \frac{C_0 - C_{DBT} - C_{TH} - C_{HH} - C_{BP} - C_{CHB} - C_{BCH}}{C_0} \times 100\% \quad (2)$$

where C_0 and C_{DBT} are the concentrations of DBT in the feed and product, whereas C_{TH}, C_{HH}, C_{BP}, C_{CHB}, and C_{BCH} are the concentrations of TH-DBT, HH-DBT, BP, CHB, and BCH, respectively.

2. Results

2.1. Characterization of the supports

The XRD patterns of Si-MCM-41, Al-MCM-41, MY(M) and MY(C) are shown in Fig. 1. Strong reflections at $2\theta = 2.2°$ were observed in the XRD patterns of all the samples, indicating that

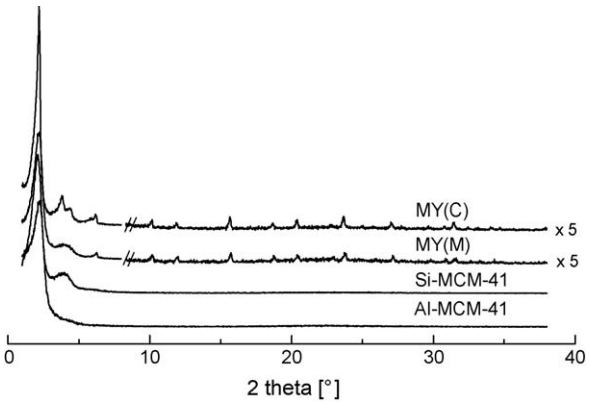

Fig. 1. XRD patterns of the supports.

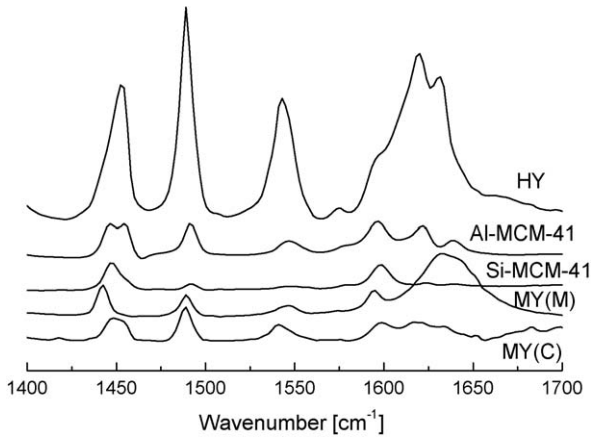

Fig. 2. Infrared spectra of pyridine adsorbed on different samples.

meso-structures were well developed. Comparison of the diffraction peaks at the high diffraction angles in the XRD patterns of MY(C) and MY(M) with the pattern of HY zeolite revealed that HY zeolite crystals were present in the samples.

The structural properties as well as SiO_2/Al_2O_3 ratios of HY, Si-MCM-41, Al-MCM-41, MY(M) and MY(C) are summarized in Table 1. Both the surface area and total pore volume of MCM-41 were decreased by the introduction of Al and HY zeolite to MCM-41, whereas the mesopore size remained almost unaffected. Due to the introduction of HY zeolite with a relative high Al_2O_3 content (SiO_2/Al_2O_3 ratio: 5), MY(M) and MY(C) showed much lower SiO_2/Al_2O_3 ratios than that of Al-MCM-41.

The morphology and pore structure of MY(C) have been investigated in our previous paper [20]. The MY(C) possessed a clearly distinguished core/shell structure with the shell thickness less than 20 nm and the MCM-41 pore channels were oriented outward from the inner HY core.

Fig. 2 shows the FT-IR spectra of pyridine adsorbed on HY, Si-MCM-41, Al-MCM-41, MY(M) and MY(C) in the region 1400–1700 cm^{-1} at 300 °C. In the spectrum of HY, the expected bands due to Lewis-bonded pyridine (1450 and 1620 cm^{-1}), Brϕnsted-bonded pyridine (1540 and 1640 cm^{-1}) and the band at 1490 cm^{-1} which can be assigned to pyridine associated with both Brϕnsted and Lewis acid sites were observed [21,24]. Besides these bands, bands due to hydrogen-bonded pyridine (1445 and 1596 cm^{-1}) were also detected in the spectra of Si-MCM-41, Al-MCM-41, MY(M) and MY(C). Si-MCM-41 showed two distinct bands due to hydrogen-bonded pyridine via surface OH groups, which are the only bands found in pure siliceous material [25]. In the spectrum for Al-MCM-41, the three kinds of bands were all present. Based on the intensities of the bands, Al-MCM-41 showed stronger Lewis acidity than Brϕnsted one. The observation is consisted with that reported elsewhere [26]. The band assigned to Brϕnsted acidity at about 1630 cm^{-1} was observed for MY(M). Its intensity became very weak in the spectrum of MY(C). This can be the result of the covering of the strong acid sites on the surface of HY by a less acidic mesoporous phase [20]. On the other hand, compared with MY(M), MY(C) showed the Lewis-bonded pyridine at around 1450 and 1620 cm^{-1}, indicating certain amount of Lewis acid sites were present in the composite. In summary, on the base of the intensities of all the bands present in the spectra of HY, MY(M) and MY(C), it suggests that the acidity of MY(M) was a bit stronger than that of MY(C), but all the two samples exhibited much weaker acidities than HY zeolite, which was in accordance with our previous study [21].

2.2. HDS of DBT

Fig. 3 shows the variations of HDS conversion (x_{HDS}), HYC conversion (x_{HYC}) and the selectivities to DDS and HYD pathways in DBT HDS with time on-stream for these supported Pd catalysts. Of all the four test catalysts, the HDS conversion determined during on-stream operation increased in following order: Pd/Si-MCM-41 < Pd/Al-MCM-41 ≈ Pd/MY(M) < Pd/MY(C). Although Si-MCM-41 possessed the highest specific surface area, Pd/Si-MCM-41 showed the lowest activity in DBT HDS, indicating that the pure siliceous mesoporous material is not a good support for noble metal catalysts. Guo et al. [7] reported a similar result that the Pt particles supported on pure siliceous SBA-15 were inactive in the HDS of 4,6-DMDBT at 300 °C and a total pressure of 5.0 MPa. Contrary to Pd/Si-MCM-41, Pd catalysts supported on the three acidic materials showed enhanced HDS activities and higher selectivities to HYD pathway, indicating the enhancement of support acidity significantly promotes the HYD route and thus the total HDS activity. On the other hand, an obvious hydrocracking reaction was observed in the HDS of DBT over the three catalysts.

Table 1
The structural properties and the ratios of SiO_2/Al_2O_3 for the supports.

Sample	BET surface area (m^2/g)	Pore volume (cm^3/g)		Pore diameter (nm)		SiO_2/Al_2O_3[a]
		Total	Micropore[b]	Mesopore[c]	Micropore[d]	
Si-MCM-41	1028	0.88	–	2.76	–	–
Al-MCM-41	823	0.66	–	2.73	–	78
MY(M)	821	0.66	0.08	2.74	0.54	26
MY(C)	761	0.61	0.07	2.74	0.56	29
HY[e]	658	0.52	0.17	–	0.52	5

[a] Determined by XRF.
[b] Calculated by *t*-plot curve.
[c] Calculated by BJH method.
[d] Calculated by SF method.
[e] The HY zeolite used in this work.

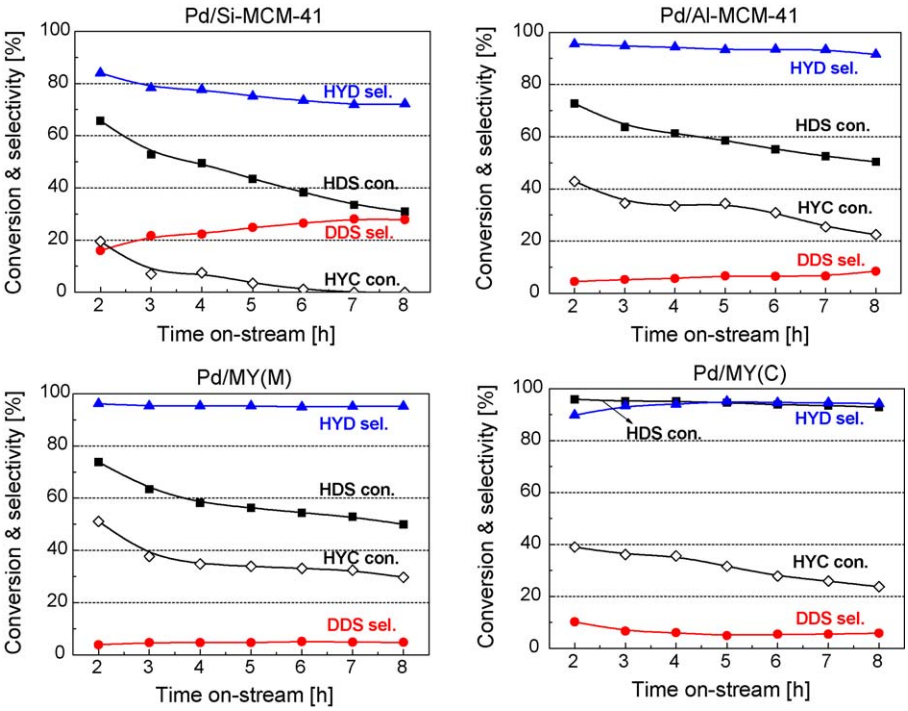

Fig. 3. The variations of HDS conversion (x_{HDS}) (■), HYC conversion (x_{HYC}) (◇) and the selectivities to DDS (●) and HYD (▲) pathways in DBT HDS with time on-stream for the supported Pd catalysts. Reaction conditions: P = 5.0 MPa, T = 300 °C, WHLV = 54 h^{-1}.

This is the result of the bifunctional catalysis involving both metal and acid centers.

To elucidate the deactivation of the four test catalysts quantitively, we defined the relative activity as the ratio of x_{HDS} at t = 8 h to that at 2 h. Therefore, the relative activity for Pd/Si-MCM-41, Pd/Al-MCM-41, Pd/MY(M) and Pd/MY(C) was 0.47, 0.69, 0.68 and 0.97, respectively. The Pd catalyst supported on the acidic support showed higher stability than that supported on the non-acidic Si-MCM-41. Among all the catalysts, Pd/MY(C) exhibited the highest HDS activity and stability. The results indicated that MY(C) with a unique core/shell structure is a promising support for Pd catalysts.

2.3. Long-term stability of Pd/MY(C)

The total DBT conversion, HDS conversion, HYC conversion, and the selectivities to DDS and HYD pathways in the long-term test over Pd/MY(C) are presented in Fig. 4. The total DBT conversion and HDS conversion decreased in the early stage after the start of reaction. After 80 h, no significant deactivation was observed for Pd/MY(C). During time on-stream operation from 80 to 110 h, the HDS performance was relatively stable. The total DBT conversion, HDS conversion and HYC conversion remained to be around 75%, 60% and 20%, respectively. The results demonstrated Pd/MY(C) had excellent stability under high space velocity (33 h^{-1}). It should be noted that more than 95% of DBT converted through HYD pathway.

3. Discussion

3.1. Effect of support acidity on the HDS performance of Pd catalysts

Although Si-MCM-41 possessed the highest surface area, Pd/Si-MCM-41 showed the lowest HDS activity and stability among the four catalysts. Moreover, no close relationship between the surface area of the support and the HDS performance of the catalyst was observed, indicating the surface area of the support or the dispersion of the catalyst may not be the key parameter affecting the HDS performance of the supported Pd catalyst. Corma et al. [12] reported Al-MCM-41-supported Pt catalyst presented the higher sulfur tolerance than the Si-MCM-41 counterpart during hydrogenation of a naphthalene feed containing 200 ppm sulfur added as DBT, despite the lower Pt dispersion of the former obtained by H_2 chemisorption. According to Tang et al. [27], the Pd dispersion of Pd/Beta-H was lower than that of Pd/Al-MCM-41 by CO chemisorption, but Pd/Beta-H exhibited higher deep hydrogenation activities of naphthalene and pyrene both in the absence and presence of 200-ppm sulfur. Besides, they also observed a higher binding energy of Pd $3d_{5/2}$ peak of Pd/Beta-H (355.5 eV) than that of Pd/Al-MCM-41 (355.0 eV), suggesting that the Pd clusters on Beta-H were "electron-deficient" compared with those of Pd/Al-MCM-41. In the present work, similar results were observed that Pd/Al-MCM-41 showed better HDS performance than Pd/Si-MCM-

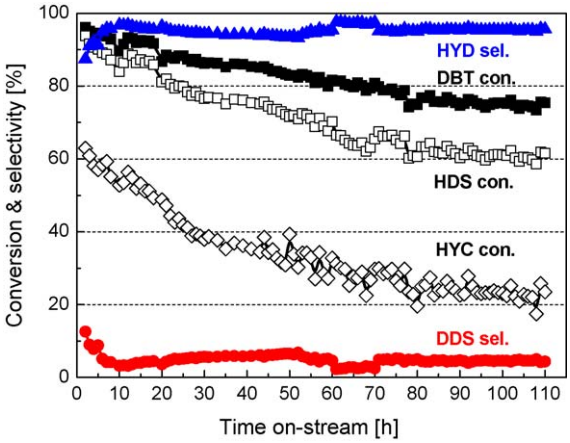

Fig. 4. The time course of total DBT conversion (■), HDS conversion (□), HYC conversion (◇), and the selectivities to DDS (●) and HYD (▲) pathways during DBT HDS over Pd/MY(C). Reaction conditions: P = 5.0 MPa, T = 300 °C, WHLV = 33 h^{-1}.

41. Therefore, it is suggested that the enhanced HDS activity of Pd/Al-MCM-41, Pd/MY(M) and Pd/MY(C) is more likely to be related to the changes in their electronic properties induced by the acidity of the support. As mentioned in Section 1, on the acidic supports, the electron-deficient metal clusters, which possess an enhanced specific catalytic activity towards hydrogenation, hydrogenolysis and a high resistance to sulfur-poisoning, may be formed [28].

Fig. 2 indicated the Al-MCM-41 possessed more Lewis acid sites than Brϕnsted ones, whereas Brϕnsted acid centers were predominated presented on the surface of MY(M). Although their surface acid properties were different, Pd/Al-MCM-41 and Pd/MY(M) exhibited a comparable catalytic performance, i.e. HDS activity, HYD selectivity and stability in DBT HDS, indicating formation of electron-deficient metal particles may not depend on the type of acid site. Gallezot [29] reported that both Brϕnsted acid sites and Lewis acid sites can be used as the potential electron acceptors. The resulting electron-deficient metal clusters can promote the π adsorption of DBT via the aromatic rings on themselves which is the prerequisite for HYD pathway [1,2]. Therefore, compared with Pd/Si-MCM-41, Pd/Al-MCM-41, Pd/MY(M) and Pd/MY(C) showed high HYD selectivity (>90%). On the other hand, the enhanced HYD selectivity may also be the result of enhanced hydrogen spillover process on the Pd catalysts supported on the acidic supports, because both the stability and the amount of spillover hydrogen are strongly dependant on the support acidity [30–34].

3.2. The structure of the support on the HDS performance of Pd catalysts

Although MY(C) showed weaker acidity than MY(M), Pd/MY(C) was much more stable than Pd/MY(M) in DBT HDS. It is suggested that the unique core/shell structure of MY(C) could be account for the superior HDS performance of Pd/MY(C). According to the structure of MY(C), Pd particles can be located on the HY core inside MY(C), in the MCM-41 coating layer, or on the outer surface of MY(C). HDS of DBT should predominantly take place on the Pd particles located in the mesopores MCM-41 coating layer, where both the diffusion and reaction of bulky DBT are readily to take place. The HDS activity of Pd on the outer surface of MY(C) is expected to be low, because they are directly exposed to DBT and H_2S, resulting in a serious poisoning. Compared with the largest opening of HY (0.74 nm) [35], the dimension of DBT (0.8 nm × 1.2 nm) is too big to diffuse into the channels of HY zeolite to reach the active sites, which means that Pd particles located on the HY core inside MY(C) are less poisoned by DBT. Although diffusion of H_2S inward the channels of HY zeolite cannot be avoided, the H_2S partial pressure in the inner HY core may not as high as that in the MCM-41 layer because of the diffusion resistance. These less poisoned Pd particles inside the MY(C) may play crucial role in promoting the HDS activity and sulfur-resistance of the supported Pd catalyst, via the so called "auto-regeneration" mechanism proposed by Song for the design of high thioresistant noble metal catalysts [36,37]. As discussed in Section 3.1, more spillover hydrogen may be generated on these less poisoned Pd particles located inside the core of MY(C) due to strong acidity of HY. These highly active hydrogen species may be transported to mesopores of the MCM-41 layer to enhance the HDS of DBT and regenerate the deactivated Pd particles by removing adsorbed sulfur [35].

Not only the sulfur resistance, but also the product selectivities were affected by the structure of the support. In the previous paper [21], we reported NiMo/MY(M) exhibited high HDS activity and HYC activity, whereas NiMo/MY(C) had an equivalent HDS activity but much lower HYC activity. The large difference between the two mixed materials supported NiMo sulfides in HYC activity may result from their pore structures. In the present work, the Pd/MY(C) also showed a lower HYC activity than Pd/MY(M), but the difference was not as significant as that between NiMo/MY(M) and NiMo/MY(C). This may result from the higher hydrogenation/dehydrogenation ability of Pd. According to the bifunctional hydrocracking reaction mechanism [38], both hydrogenation and dehydrogenation are necessary. Therefore, it is reasonable that Pd catalyst with high hydrogenation and dehydrogenation activities exhibits a high hydrocracking activity than its NiMo counterpart. In the case of Pd/MY(C), the desulfurized products (CHB and BCH) were difficult to diffuse deep into the micropores of the HY zeolite in the inner-core of MY(C), which can be account for its low HYC activity compared with that of Pd/MY(M).

In the case of noble metal catalysts employed in HDS reaction, it is generally accepted that the deactivation was attributed to sulfur-poisoning. By means of ^{35}S radioisotope tracer method, Kabe et al. found the sulfided Pd or Pt species supported on alumina were presented in the form of PdS_x or PtS_x (x = 0–0.25) in low H_2S partial pressure, and all the sulfur incorporated into noble metal particles were almost labile sulfur, participating in sulfur cycle in DBT HDS [39,40]. Barrio et al. [11] investigated the variations of the Pd $3d_{5/2}$ binding energy (BE) of Pd/ASA before and after DBT HDS. An increase in the BE values (about 0.4 eV) was observed upon on-stream operation, suggesting the loss of the metal character of Pd due to partial sulfidation of Pd. Therefore, the remarkable deactivation of Pd/MY(C) in the early stage was probably attributed to the slow partial sulfidation of Pd particles. However, the activity was rather stable after 80 h, indicating the surface sulfidation could slowdown or equilibrium between sulfidation of Pd and reduction of PdS_x was reached. In addition, the partial sulfidation of Pd in the early stage was also confirmed by the decrease in the hydrocracking activity of Pd/MY(C) (Fig. 4), because PdS_x possesses lower hydrogenation activity than Pd.

4. Conclusions

The HDS performances of the supported Pd catalysts are significantly influenced by the properties of the supports. Pd catalysts supported on the acidic supports showed enhanced stability as well as HDS and HYD activities. Among the catalysts studied, Pd/MY(C) exhibited the highest activity and stability in DBT HDS. Its enhanced HDS performance especially sulfur resistance may result from the unique core/shell structure of MY(C). Due to small pore size of HY zeolite relative to DBT molecule and diffusion resistance, Pd particles located on HY in the core of Pd/MY(C) can be less affected by DBT and H_2S. Over these Pd particles, more spillover hydrogen may be generated due to strong acidity of HY and transported to mesopores of the MCM-41 layer to enhance the HDS of DBT and regenerate the deactivated Pd particles by removing adsorbed sulfur.

Acknowledgements

The authors acknowledge the financial supports from the Natural Science Foundation of China (20333030, 20503003, and 20773020), the Education Ministry of China (20030141026), NCET, and the "111" Project. The authors are grateful to Mr. J. Ren and Ms. D. Hou for their kind help.

References

[1] C. Song, Catal. Today 86 (2003) 211.
[2] S. Bej, S. Maity, U. Turaga, Energy Fuels 18 (2004) 1227.
[3] N. Kunisada, K.-H. Choi, Y. Korai, I. Mochida, K. Nakano, Appl. Catal. A 269 (2004) 43.
[4] A. Niquille-Röthlisberger, R. Prins, J. Catal. 242 (2006) 207.
[5] A. Niquille-Röthlisberger, R. Prins, Catal. Today 123 (2007) 198.

[6] Y. Sun, R. Prins, Angew. Chem. Int. Ed. 47 (2008) 8478.
[7] H. Guo, Y. Sun, R. Prins, Catal. Today 130 (2008) 249.
[8] Y. Yoshimura, M. Toda, T. Matsui, M. Harada, Y. Ichihashi, K.K. Bando, H. Yasuda, H. Ishihara, Y. Morita, T. Kameoka, Appl. Catal. A 322 (2007) 152.
[9] H. Yasuda, T. Sato, Y. Yoshimura, Catal. Today 50 (1999) 63.
[10] T. Fujikawa, K. Idei, T. Ebihara, H. Mizufuchi, K. Usui, Appl. Catal. A 192 (2000) 253.
[11] V.L. Barrio, P.L. Arias, J.F. Cambra, M.B. Güemez, B. Pawelec, J.L.G. Fierro, Catal. Commun. 5 (2004) 173.
[12] A. Corma, A. Martínez, V. Martínez-Soria, J. Catal. 169 (1997) 480.
[13] X. Bai, W.M.H. Sachtler, J. Catal. 129 (1991) 121.
[14] W.M.H. Sachtler, Acc. Chem. Res. 26 (1993) 383.
[15] K. Thomas, C. Binet, T. Chevreau, D. Cornet, J.-P. Gilson, J. Catal. 212 (2002) 63.
[16] T. Tang, C. Yin, L. Wang, Y. Ji, F. Xiao, J. Catal. 249 (2007) 111.
[17] K.R. Kloetstra, H.W. Zandbergen, J.C. Jansen, H. van Bekkum, Micropor. Mater. 6 (1996) 287.
[18] M. Hartmann, Angew. Chem. Int. Ed. 43 (2004) 5880.
[19] Y. Fang, H. Hu, J. Am. Chem. Soc. 128 (2006) 10636.
[20] X. Li, F. Zhou, A. Wang, L. Wang, Y. Hu, Ind. Eng. Chem. Res. 48 (2009) 2870.
[21] J. Ren, A. Wang, X. Li, Y. Chen, H. Liu, Y. Hu, Appl. Catal. A 344 (2008) 175.
[22] E. Campaigne, L. Hewitt, J. Ashby, J. Heterocycl. Chem. 553 (1969) 6.
[23] A. Wang, T. Kabe, Chem. Commun. (1999) 2067.
[24] E.P. Parry, J. Catal. 2 (1963) 371.
[25] B. Chakraborty, B. Viswanathan, Catal. Today 49 (1999) 253.
[26] R. Mokaya, W. Jones, Z. Luan, M.D. Alba, J. Klinowski, Catal. Lett. 37 (1996) 113.
[27] T. Tang, C. Yin, L. Wang, Y. Ji, F. Xiao, J. Catal. 257 (2008) 125.
[28] W.M.H. Sachtler, A.Y. Stakheev, Catal. Today 12 (1992) 283.
[29] P. Gallezot, Catal. Rev. Sci. Eng. 20 (1979) 121.
[30] S.D. Lin, M.A. Vannice, J. Catal. 143 (1993) 539.
[31] S.D. Lin, M.A. Vannice, J. Catal. 143 (1993) 554.
[32] S.D. Lin, M.A. Vannice, J. Catal. 143 (1993) 563.
[33] M. Sugioka, F. Sado, T. Kurosaka, X. Wang, Catal. Today 45 (1998) 327.
[34] X. Li, A. Wang, Z. Sun, C. Li, J. Ren, B. Zhao, Y. Wang, Y. Chen, Y. Hu, Appl. Catal. A 254 (2003) 319.
[35] H. Zhang, X. Meng, Y. Li, Y.S. Lin, Ind. Eng. Chem. Res. 46 (2007) 4186.
[36] C. Song, Chemtech 29 (1999) 26.
[37] C. Song, X. Ma, Appl. Catal. B 41 (2003) 207.
[38] P.B. Weisz, Adv. Catal. 13 (1962) 137.
[39] T. Kabe, W. Qian, Y. Hirai, L. Li, A. Ishihara, J. Catal. 190 (2000) 191.
[40] E.W. Qian, K. Otani, L. Li, A. Ishihara, T. Kabe, J. Catal. 221 (2004) 294.